Bioactive Materials 3 (2018) 174–185

Contents lists available at ScienceDirect

Bioactive Materials

journal homepage: http://www.keaipublishing.com/en/journals/bioactive-materials/

Magnesium degradation under physiological conditions – Best practice

Jorge Gonzalez, Rui Qing Hou, Eshwara P.S. Nidadavolu, Regine Willumeit-Römer, Frank Feyerabend*

Institute of Materials Research, Division Metallic Biomaterials, Helmholtz-Zentrum Geesthacht, Max-Planck-Str. 1, 21502 Geesthacht, Germany

ARTICLE INFO

Article history:
Received 20 December 2017
Received in revised form
15 January 2018
Accepted 15 January 2018
Available online 14 February 2018

Keywords:
In vitro
Flow conditions
Degradation products
Cell culture conditions

ABSTRACT

This review focusses on the application of physiological conditions for the mechanistic understanding of magnesium degradation. Despite the undisputed relevance of simplified laboratory setups for alloy screening purposes, realistic and predictive *in vitro* setups are needed. Due to the complexity of these systems, the review gives an overview about technical measures, defines some caveats and can be used as a guideline for the establishment of harmonized laboratory approaches.

1. Introduction

Research about degradable magnesium alloys is of increasing interest for material scientists, biologists and clinicians. As the first products are already clinically available [1], a higher awareness of this topic has been achieved. Unfortunately, not too many research groups are interested in getting a mechanistic insight into the underlying processes due to the high complexity of the degradation process under physiological conditions. A main reason for this is the comparably aggressive environment – salt-containing fluids, the presence of sugars and proteins and the application of cell culture conditions. Moreover, one additional quite difficult aspect is to keep sterility of the systems.

1.1. Why are physiological conditions so important?

The easiest and most astonishing experiment to prove this specific importance is the direct observation of the sample morphology after immersion in pure/deionized water and cell culture conditions (Fig. 1). While the samples under atmospheric conditions exhibit a black surface, typically consisting of $Mg(OH)_2$, the samples immersed under cell culture conditions show many precipitates, which could be identified as $MgCO_3$ [2,3]. Additionally, the introduction of cell culture conditions accelerates the degradation rate of all materials, as monitored by the increase of osmolality.

Despite the fact that cell-based experiments are conducted under physiological conditions, the environment has a considerable influence on the degradation behaviour of various materials. This is not only applicable to degradable metals (i.e. magnesium, iron, zinc, tungsten), but also to degradable polymers. As it was stated in a leading opinion paper [4], even for general testing of materials physiological conditions should be applied when using, e.g. simulated body fluids.

In the case of degradable materials, this is even more interesting, as a continuously changing interface between material and cells is developing over time. To understand this development is of utmost importance in this research area. Also, the biological clues (e.g. cellular communication, the interaction of various cell types, material – protein interactions) have to be analysed, as they additionally will have an impact on the material degradation.

This manuscript aims to give an overview about physiological experimental setups, state some caveats and to help harmonising laboratory approaches.

2. Simulated or not? The question of appropriate conditions

To choose a suitable physiological solution, it is a critical point to

* Corresponding author.
E-mail address: frank.feyerabend@hzg.de (F. Feyerabend).
Peer review under responsibility of KeAi Communications Co., Ltd.

https://doi.org/10.1016/j.bioactmat.2018.01.003

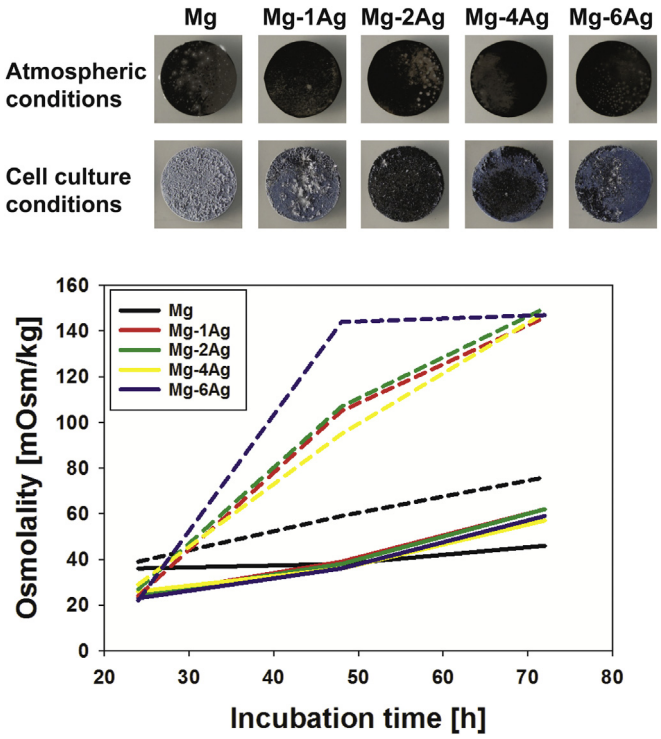

Fig. 1. Upper panel: optical morphology of different materials (10 mm diameter) after 72 h incubation in distilled water. **Lower panel:** Measurement of the change of osmolality during the 72 h immersion. Solid lines: experiment performed under atmospheric condition, dashed lines: cell culture conditions (PhD thesis Die Ti, unpublished results).

evaluate the degradation of Mg alloys and to obtain comparable *in vitro* results to *in vivo* tests. Simulated physiological solutions with increasing complexity were used to determine the degradation of Mg: from 0.9% NaCl solution, Hanks balanced salt solution (HBSS), simulated body fluid (SBF), to cell culture medium. Different simulated solutions used result not only in different degradation rates of Mg [5], but also different degradation products [6,7], suggesting different degradation pathways and degradation mechanism. Therefore, the choice of a suitable solution for the evaluation of Mg degradation is of utmost importance.

When a Mg alloy is immersed in a physiological medium, the contact between the fresh surface and an electrolyte-containing aqueous medium lead to higher initial corrosion rates. This process involves the release of hydrogen and the alkalinization of the environment as the net reaction shows:

$$\textit{Anodic reaction}: \quad Mg \rightarrow Mg^{2+} + 2e^{-} \tag{1}$$

$$\textit{Cathodic reaction}: \quad 2H_2O + 2e^{-} \rightarrow 2OH^{-} + H_2\uparrow \tag{2}$$

$$\textit{Overall reaction}: \quad Mg + 2H_2O \rightleftharpoons Mg^{2+} + 2OH^{-} + H_2\uparrow \tag{3}$$

The formed $Mg(OH)_2$ is the first product in the degradation process and readily precipitates because of its low solubility of 12 mg/L in water. The strengthening and dissolution of this layer depend further on the other elements present in the electrolyte and the time of immersion. However, it has been shown that MgO, $Mg(OH)_2$ and $MgCO_3$ are the main degradation products formed with the application of HBSS, SBF and Dulbecco's modified eagle medium (DMEM) [3,8]. Additionally, the solubility of the various phases is dependent on environmental factors like temperature, pH and magnesium dissolution [2].

A suitable simulated solution, therefore, should contain three essential parts: appropriate inorganic ingredients, a buffering system and organic components. The detailed compositions of several common simulated physiological solutions and plasma are compared in Table 1 with the blood plasma composition. There are some reports to study the degradation of Mg in physiological saline (0.9% NaCl) solution [9,10], but they will not be discussed, as the results obtained with physiological saline solutions are far away or even contradictory from that obtained under physiological conditions [11]. To gain closer physiological conditions results, simulated body fluids (SBF) and Hanks' solution are widely used to determine the degradation rate of Mg, as they have a similar inorganic ion composition compared to plasma. SBF was developed as a solution for *in vitro* measurement of apatite-forming ability on implant materials and several improved recipes are available (Technical Committee ISO/TC150) [12,13]. Therefore it is of utmost importance to state the exact composition or to cite the original publication in the materials and methods part as a guide for the readers [14]. Compared with other solutions showed in Table 1, SBF has a closer composition to plasma. However, a significant amount of Ca and Mg ions present in plasma is bound to proteins, which should be taken into consideration due to the absence of organic compounds in SBF. Moreover, Ca^{2+} ions in combination with a high concentration of HCO_3^- can largely affect the degradation behaviour of Mg under cell culture condition [15].

Another critical parameter is the buffering system. A good simulated body solution should possess the similar buffering capacity to that of body plasma. Blood pH is regulated by (a) the open system HCO_3^-/CO_2 adjusted by the respiration via the lungs, (b) plasma protein buffers (HPr/Pr^-) and (c) a low concentration of phosphate [12]. However, the most common buffers for simulated body fluids used are (a) 4-(2-hydroxyethyl)-1-piperazineethanesulfonic acid (HEPES), (b) Tris-HCl, (c) $CO_2/NaHCO_3$ and (d) phosphate. HEPES and TRIS were introduced in the 1960's by Good et al. [32] for systems without CO_2-buffering.

The phosphate buffering contribution in human body is low and only significant in the urine and in the intracellular fluid, due to its low concentration. The too high concentration of phosphate alters the chemical properties of the corrosion layer, as they can produce insoluble salts with magnesium ions and eventually precipitating on the surface, thereby leading to a different degradation performance compared to *in vivo* conditions [31,33]. Therefore, PBS is not suitable to simulate or predict degradation behaviour of Mg alloys under *in vivo* conditions. In addition, PBS also should be avoided for live/dead experiment or critical point drying due to the change of surface condition, as shown in Fig. 2.

Under the same conditions, HEPES increases the corrosion rate of pure Mg by a factor of up to four times compared with $NaHCO_3$ buffering alone not only in simple salt solutions but also in EBSS and DMEM [7,25,34–36]. For WZ21 alloy, this factor increased to approximately 60 in SBF buffered with HEPES (100 mmol/L) compared with that buffered with $CO_2/NaHCO_3$ [18]. Moreover, HEPES in testing solutions reduces the formation of calcium phosphate and carbonate in the degradation layer by influencing the nucleation processes [25,34]. Therefore, HEPES destabilises the protective layer, generating a less dense degradation layer and allowing the progressive diffusion of aggressive ions like Cl^- [37]. Also on glass-ceramics it was shown that HEPES leads to a selective dissolution of Ca-containing phases and is therefore also for this class of degradable materials not recommended [38].

Tris is also one common buffering used in simulated body fluid, which also accelerates the degradation rate of pure Mg by a factor of ten during earlier stage exposure due to the consumption of OH^- [39]. Moreover, when Tris-HCl is present in SBF, pure magnesium is

Table 1
Compositions of common simulated physiological solutions. Addition of organic components are highlighted in bold.

Ingredient	Simulated blood plasma (SBP)	SBF	Hank's	Earle's Balanced Salt Solution (EBSS)	Kirkland's biocorrosion medium (KBM)	DMEM	E-MEM	MEM	Blood Plasma (Dissociated concentration)
Na^+	120.89	142.0	141.6	151	120.3	155.3	151	144.4	142
K^+	5.37	5.0	5.4	5.4	5.0	5.3	5.4	5.3	5.0
Ca^{2+}	1.80	1.6–2.5	1.3–2.5	1.8	2.5	1.8	1.8	1.8	2.5 (1.3)
Mg^{2+}	0.87	1.0–1.5	0.75–0.87	0.4	0.5	0.8	0.8	0.8	1.5 (1.0)
Cl^-	125.2	103–148.8	144–147	135	102.5	115.7	125	126.2	103
HCO_3^-	2.6	4.2–27	4.2	26.2	26.2	44.1	26.2	26.2	22–30
HPO_4^{2-}	1.14	1.0	0.3	1	0.9	0.9	0.9	1.0	1.0
$H_2PO_4^-$			0.4						
SO_4^{2-}	0.87	0.5	0.26–0.8	0.4	0.5	0.8	0.8	0.4	0.5
Amino acids	–	–	–	–	–	**10.60**	**0.86 (mg/L)**	**8.54**	**unknown**
Vitamins	–	–	–	–	–	**0.15**	–	**0.32**	**unknown**
Proteins (g/L)	–	–	–	–	–	–	–	–	**63–80**
Dex/glucose (g/L)	–	–	**5.6**	**5.5**	**5**	**25**	**1**	**5.5**	**3.6–5.2**
Phenol red (g/L)	–	–	–	–	–	**0.04**	**0.1**	**0.03**	–
Reference	[5]	[12,16–20]	[5,21–24]	[20,25]	[25]	[26–28]	[7]	[29,30]	[7,12,25,31]

Note: All concentrations in mmol/L unless otherwise stated.

more sensitive to pitting corrosion [16]. Similar to HEPES it was shown for AZ31 alloys that Tris-HCl prevents the formation of precipitates and degradation products due to the lower local pH [40]. For WZ21 alloy, the corrosion rate is five times higher in SBF buffered with 50 mmol/L Tris than that buffered with CO_2/HCO_3^- [18]. Even when the CO_2/HCO_3^--buffered SBF shows a lower pH than Tris/HEPES buffered SBF, the degradation rate of pure Mg in SBF buffered with CO_2/HCO_3^- is the lowest compared to the other buffered SBFs [18]. This indicates an increase of Mg degradation caused by the addition of HEPES or Tris (as a pH buffer) results not only from the lower pH on Mg surface; also possible unidentified interactions between HEPES/Tris and Mg.

It is not surprising that due to the similarity to the human pH regulation system, the CO_2/HCO_3^- buffering system is preferable for *in vitro* tests instead of HEPES and Tris. The presence of this buffering system causes the shift of equilibrium towards the HCO_3^-, leading to the formation of carbonates of ACO_3 type (A- Alkali metals: lithium (Li, if used as alloying element), sodium (Na), and potassium (K)). The inclusion of CO_2 to the testing system lead to a more stable pH via the equilibrium of HCO_3^-/CO_2, also promotes the formation of carbonate on magnesium surface. Under aqueous conditions, the presence of CO_2 results in the formation of a carbonated film, which is thicker than magnesium hydroxide film formed in the absence of CO_2, resulting in a slower corrosion [41]. Increase of bicarbonate concentration in SBF from 4 (interstitial fluid content) to 27 mmol/L (blood plasma content) is proven to increase the passivity of the degradation layer and reduce corrosion [42]. However, when the bicarbonate concentration increase above 40 mmol/L in SBF, the degradation shows a reversed trend [43]. The dissociation of bicarbonate into hydrogen protons further undermines the formed $Mg(OH)_2$ layer, which is expected to be the reason for the increased degradation. In contrast when proteins are present, Agha et al. found that $NaHCO_3$ (4.2, 22, 44 mmol/L) alone does not influence significantly the degradation rate of pure Mg in HBSS + 10% FBS under cell culture conditions, indicating an equilibrium of HCO_3^-/CO_2 buffering system [15]. At present, many studies were performed under cell culture conditions (5% CO_2, 21% O_2, 95% relative humidity), which also was discussed as physiological environment [27,28]. To ensure the dissolution of the CO_2 in the testing solution, a set-up with flow conditions for CO_2 in the testing container was used in degradation tests [18,21,23,24]. The inflow of CO_2 enhance their contact with the testing solution, thereby increasing the dissolution. Zainal Abidin et al. stressed the importance of the partial pressure of CO_2 used according to the concentration of HCO_3^- in testing solution, to maintain the pH in the testing solution constant [21]. The resulting pH under cell culture conditions is directly correlated to the amount of HCO_3^- and the partial pressure of CO_2 in the incubator (Fig. 3).

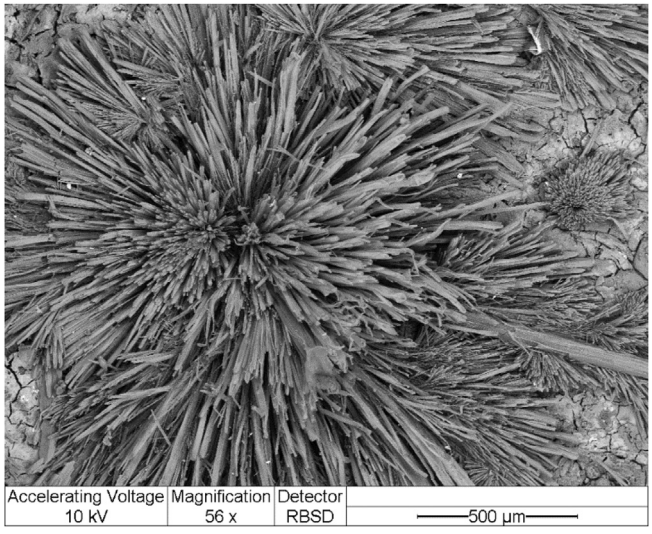

Fig. 2. Morphology of Mg-4Y sample after critical point drying with PBS-containing ethanol.

Sulphate ion concentration in SBF tends to accelerate corrosion to some degree during initial stages of immersion [46]. In another study, the addition of magnesium sulphate (200 mg/L) to HBSS+10% FBS did not show any considerable influence on degradation except for creating heterogeneity in the degradation layer [47]. Phosphate buffered SBF increased the corrosion resistance of Mg-Mn and Mg-Mn-Zn alloys [48]. However, Ca/P ratio in this study was much lower than that of hydroxyapatite and the decrease in degradation rate was attributed to the formation of an amorphous Mg rich phosphate layer.

Organic components play a considerable role in the degradation of Mg, especially for the biological performance of Mg. In addition, the plasma proteins are a vital part for physiologic pH regulation [49]. For a full understanding of Mg degradation process under physiological conditions, proteins are essential constituents to include for *in vitro* investigations. They affect not only the degradation rate, but also the degradation products [7,50]. Although the underlying mechanism is still unclear, the evident influence of organic components on degradation behaviour has already been

stated [51,52]. One recent modeled mechanism of magnesium degradation is the iron impurity-based re-deposition effect [53]. In a further study the inhibition efficiency of iron-complexing agents was analysed, also with the view on *in vitro* testing of magnesium alloys for biomedical applications [54]. In this study, corrosion inhibiting effects of folic acid, ascorbic acid and glucose were determined, whereas Tris, D-panthenol, streptomycin and penicillin accelerated corrosion markedly. However, the primary iron-binding entities in physiological condition are proteins. The abundance of proteins in blood has been detected by proteomic approaches, revealing 490 proteins present [55]. Of these, albumin is the most abundant protein, and it has been shown that it has a substantial iron-binding capacity, although the binding is only weak [56]. The class of beta-globulins, containing fibrinogen and transferrin are also highly abundant. Transferrin is a dedicated protein for iron-transport and has a high affinity to bind iron [57,58]. Fibrinogen has a function as acute phase protein and is essential for iron regulation [59,60]. This, in turn, is another hint why there are big discrepancies between results obtained from more "technical" setups and *in vivo* conditions. Therefore, it might be promising to use the CO_2 buffer system in combination with protein-containing solutions to exclude the possible influence of pH changes and to gain a physiological condition.

Walker et al. [35] compared the degradation rate of pure Mg and five alloys (AZ31, Mg-0.8Ca, Mg-1Zn, Mg-1Mn, Mg-1.34Ca-3Zn) under *in vivo* conditions (in a subcutaneous environment in Lewis rats) with different *in vitro* media (EBSS; MEM, MEM+40 g/L BSA) buffered by CO_2/HCO_3^-. The degradation rate of samples in EBSS was comparable to *in vivo* conditions, and the addition of BSA to MEM increased the degradation rate of Mg and Mg alloys in this study. A.H. Martinez Sanchez et al. reviewed the comparison between *in vitro* and *in vivo* results [61]. This review shows that the corrosion factors for Mg alloys are below 3 for EBSS and SBF, while it is in the range between 1.5 and 3.5 for MEM. The corrosion factor increases to a range between 4 and 7 when proteins (BSA) are added. Therefore, from the point of view of degradation rate prediction, EBSS and SBF are better choices for the *in vitro* degradation. This simplified approach is suitable for material screening purposes. However, it should be kept in mind, that also the degradation rates *in vivo* are highly dependent on the locus of implantation [62].

Although, the degradation products were not considered in these studies, the formation of different products indicates different degradation process and possible different mechanism. Marco et al. [26] investigated the degradation behaviour of pure Mg, Mg-10Gd and Mg-2Ag in HBSS, PBS and DMEM under cell culture conditions. Compared with *in vivo* tests, DMEM as testing medium, not only maintains a physiological pH level and produces a comparable degradation rate to *in vivo* conditions, but also generates the degradation layer similar to that formed *in vivo*. Moreover, the addition of FBS to cell culture media always slows down the degradation of Mg alloys [7,50,51,63,64]. Similar results were obtained for iron-based materials, where the introduction of CO_2 in the presence of HBSS lead to different degradation products and patterns [65]. Therefore, cell culture media with FBS, such as, DMEM; MEM, Alpha-MEM, combined with the CO_2/HCO_3^- buffering, are proposed to use for *in vitro* investigation for Mg and other biodegradable materials.

In summary, how to choose an appropriate solution for *in vitro* investigation is depending on the intention of the investigation. Herein, SBF and EBSS in combination with CO_2/HCO_3^- buffering are suggested for screening materials and comparing the degradation rate. Whereas, for the study of the degradation behaviour and mechanisms involved, cell culture media with FBS (MEM, DMEM, α-MEM) are recommended to obtain a comparable degradation behaviour to *in vivo* conditions, although they represent a much more complex system, higher technical and experimental effort, and are not standard equipment in material science oriented laboratories. As an overview, the current knowledge about degradation products under physiological conditions is depicted in Fig. 4.

3. To flow or not to flow? The question of experimental setups

The difficulty in monitoring the *in vivo* environmental conditions during magnesium materials degradation has been hindered the identification of relevant parameters to be translated into a more realistic *in vitro* set-up. Nevertheless, previously compiled information about specific fluid content and blood flow in relevant human tissues [62] seem to correlate with differences in the degradation rate founded by μCT for different implant parts in contact with different tissues [72,73]. These findings point to the need of addressing the hydrodynamic conditions surrounding the

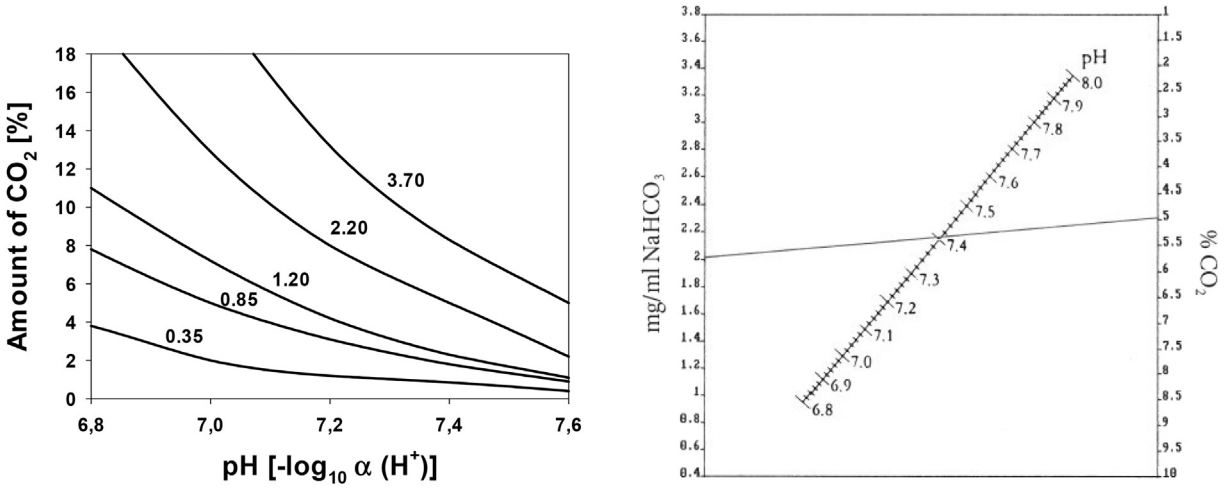

Fig. 3. Left: Dependence of buffering pH on the amount of $NaHCO_3$ (in g/L; inserts) under cell culture conditions at different CO_2 regimes (adapted from Ref. [44]). Right: simplified nomogram for the determination of CO_2 according to the concentration of $NaHCO_3$ in the medium based on acid-base calculations [45]. The line depicts as an example the normal range of CO_2 and $NaHCO_3$ concentrations in cell culture conditions.

tested material with the aim of generating comparable results and progress into the mechanisms involving magnesium degradation under physiological conditions.

Evaluation of the hydrodynamic conditions is needed due to their ability to modulate the rate constant of electrochemical processes. Fig. 5 displays the surface electrochemical and chemical processes involved in magnesium degradation including the necessary mass transfer processes between the surface region and the bulk solution. As a consequence of this mass transfer process and the natural tendency of a fluid to stick to a solid surface, a gradient of reactants (e.g. H_2O) and products (e.g. Mg^{2+} and OH^-) is stabilised [74]. Depending on the hydrodynamic conditions, the contribution of the mass transfer can be a major rate-determining step regarding the overall degradation process.

Several attempts focused recently on the enhancement of standardisation of *in vitro* setups for degradable materials [75,76]. This was due to the application of a multitude of set-ups, which complicate the evaluation of degradation rate or degradation mechanisms of magnesium alloys (Table 2).

The currently applied testing methodologies can be divided into two categories; (1) those performed under static conditions, and (2) those performed under dynamic conditions.

Under static conditions degradation analysis is performed in the same medium during the whole immersion time [91] or by entirely or partially replacing it with fresh medium during the immersion time (semi-static) [7,100,102]. In these cases, mass transfer between the surface region and the bulk medium is controlled by the processes of migration, diffusion and a certain degree of convection generated by the H_2 evolution from the surface according to the cathodic reaction (Equation (2)).

Dynamic conditions [106] involve the immersion of the material at a constant or intermittent flow rate of the degradation medium. The exchange of mass between the surface region and the bulk is accelerated in this case by an increase in the convective participation due to the flow applied.

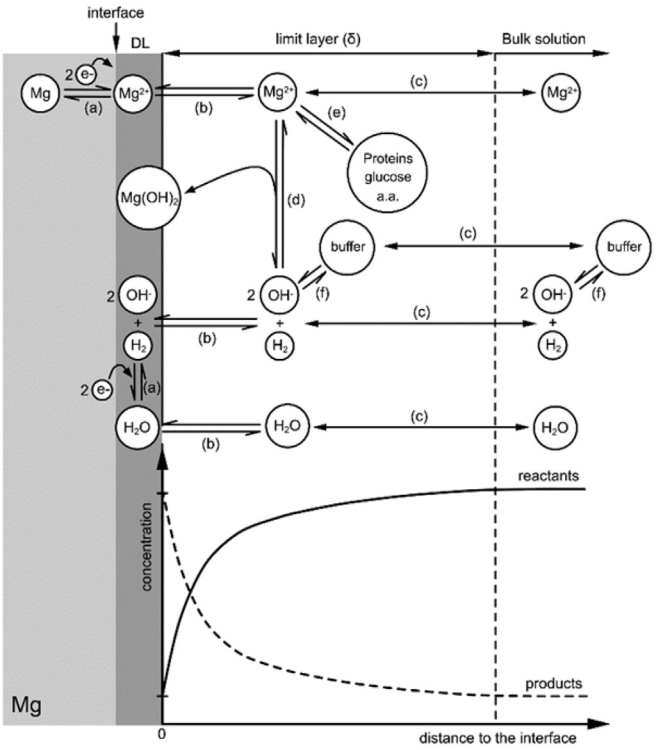

Fig. 5. Schematic description of the degradation process (adapted from Ref. [77]) involving; (a) electrochemical reactions, (b) absorption-desorption processes, (c) mass transfer processes, (d) precipitation reactions, (e) complexation reaction, (f) acid-base reactions.

3.1. Caveats for static conditions

The available standards are proposing certain volume to surface (V/A) ratios for immersion tests [109,110]. The notable difference in

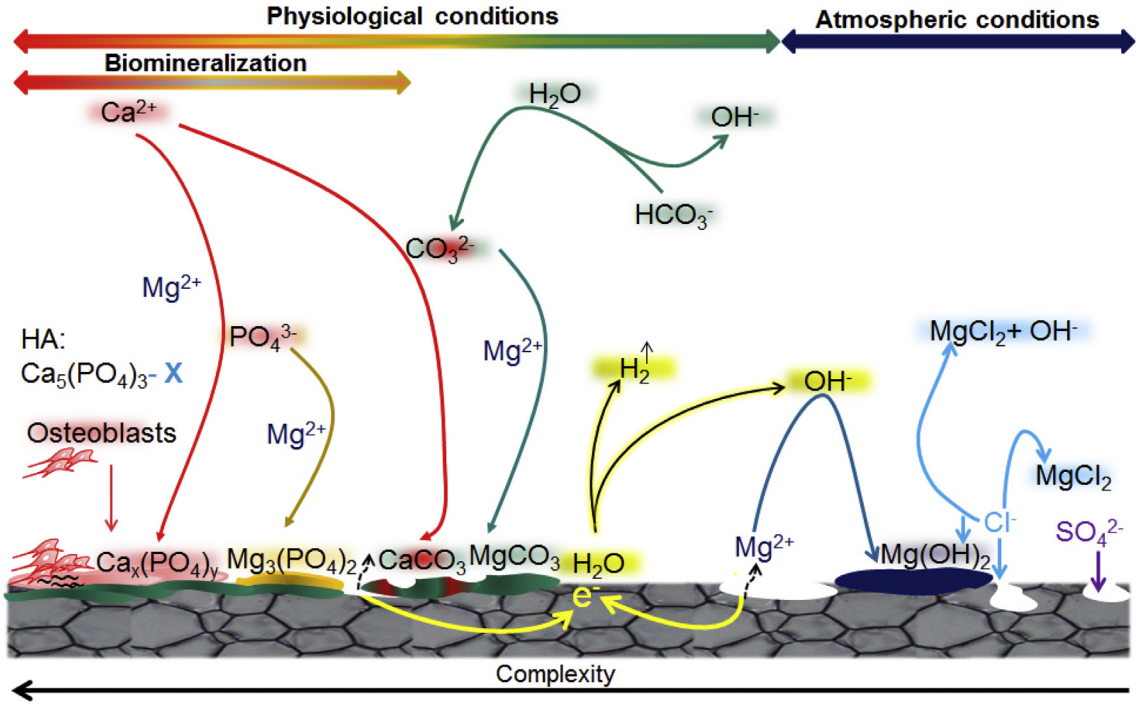

Fig. 4. Degradation products formed under physiological conditions and the corresponding chemical reactions. Data are compiled from Refs. [7,50,66–71].

Table 2
Compilation of published immersion tests set-ups used in the characterisation of Mg materials degradation. Studies performed under physiological conditions are highlighted in bold. Abbreviations: AC: Atmospheric conditions; CCC: Cell Culture Conditions (37 °C, 5% CO_2, 95% rH); HBSS: Hank's Balanced Salt Solution; SBF: Simulated Body Fluid; DMEM: Dulbecco's Modified Eagle Medium; FBS: Foetal Bovine Serum; EMEM: Eagle's Minimum Essential Medium; BSA: Bovine Serum Albumin; MEM: Minimum Essential Medium; m-SBF: modified Simulated Body Fluid; PBS: Phosphate Buffered Saline; GibcoTM Glutamax®: standardised addition of L-alanyl-L-glutamine; EBSS: Earle's Balanced Salt Solution; P/S: Penicillin/Streptomycin; PEO: Plasma Electrolytic oxidation coating process; HAp: Hydroxyapatite coating; OCP: Octacalcium phosphate coating; PM: Powder metallurgy processing; n/a: data not available.

Method	Alloy	Medium	Conditions	V/A ratio (mL/cm^2)	Medium exchange	Immersion time	Flow rate/FISS	Reference
Static	Mg-Mn-Zn	HBSS, SBP	AC	0.67, 6.67 and 66.7	–	300 h	–	[5]
Static	Mg-Ca, AZ31, AZ91	HBSS, DMEM, DMEM + FBS	AC	Not reported	–	7 days	–	[78]
Static	**Pure Mg**	**EMEM**	**CCC**	**0.17**	–	**24 h**	–	[79]
Static	Mg-Ca	NaCl + BSA	AC, 37 °C	88	–	1, 2, 12 h	–	[80]
Static	Mg-Ca	HBSS, MEM, MEM + FBS	AC, 37 °C	300	–	n/a	–	[81]
Static	AZ31	Modified HBSS	AC, 37 °C	25–50	–	72, 90 h	–	[82]
Static	M1A	SBF, SBF + BSA	AC, 37 °C	Not reported	–	1–24 h	–	[83]
Static	**Pure Mg**	**DMEM**	**CCC**	**5000**	–	**16 days**	–	[84]
Static	Pure Mg (PM)	DMEM	AC, 37 °C	378	–	1 h	–	[34]
Static	AZ31, AZ31-Lu	NaCl	AC	80	–	7 days	–	[85]
Static	Pure Mg	Artificial saliva	AC, 37 °C	25	–	10 days	–	[86]
Static	AM50, AM50-PEO	m-SBF	AC, 37 °C	14.5	100%/3 days or when pH ≥ 8.0	60 days	–	[87]
Static	Pure Mg	NaCl + glucose, HBSS + glucose	AC, 37 °C	30	–	60 h	–	[88]
static	AZ31, AZ31-Hap, AZ31-OCP	EMEM+10%FBS	AC	50	–	14–52 weeks	–	[89]
Static	Pure Mg, Mg-4Y-3RE, Mg-5Gd, Mg-10Gd, Mg2Ag, Mg4Ag, Mg6Ag	PBS. DMEM Glutamax	AC, 37 °C/CCC	30	–	95–160 h	–	[90]
Static	**Pure Mg, Mg-4Y-3RE, Mg-5Gd, Mg-10Gd, Mg-2Ag, Mg-4Ag, Mg-6Ag**	**DMEM Glutamax**	**CCC**	**30–50**	–	**100–200 h**	–	[91]
Static	WE43-Hf	SBF/37 °C	AC, 37 °C	20	–	1 day	–	[92]
Static	Mg-3Sn-1Zn-0.5Mn	SBF	AC, 37 °C	25 (ASTM G31-72)	–	30 days	–	[93]
Static	Pure Mg	0.9% NaCl + L-cysteine + glucose	AC, 37 °C	30	–	72 h	–	[94]
Static	**WE43**	**HBSS**	**CCC**	**30–62**	–	**72 h**	–	[95]
Semi-static	**Pure Mg**	**NaCl, EBSS, EMEM**	**CCC**	**13.7**	**55%/day**	**15 d**	–	[7]
Semi-static	WE43	SBF	AC, 37 °C	15	100% Regularly not specified (to avoid pH > 8.0)	30 days	–	[96]
Semi-static	**Pure Mg**	**DMEM Glutamax (0,10, 20% FBS), HBSS (0, 10, 20% FBS), H_2O (Milipore water)**	**CCC**	**Not reported**	**100%/2–3 days**	**3 d**	–	[70]
Semi-static	Mg-Nd-Zn-Zr	SBF	AC, 37 °C	30 (ASTM G31-72)	100%/day	120 h	–	[97]
Semi-static	Pure Mg, Mg-0.8Ca, Mg-1Zn, Mg-1Mn, Mg-1.34Ca-3Zn	EBSS, MEM, MEM + BSA	CCC, AC, 37 °C/HEPES	13.4 (stirring)	55%/day	7, 14, 21 d	n/a	[98] {Walker, 2012 #2}
Semi-static	**Pure Mg, WE43, E11**	**HBSS(+10% FBS), DMEM Glutamax (+10% FBS)**	**CCC**	**0.2**	**100%/day**	**3 d**	–	[99]
Semi-static	AZ31B	NaCl, SBF	C, 37 °C	330	100%/day	1, 3, 10 d	–	[100]
Semi-static	**Pure Mg, Mg-xCa, Mg-xMn, Mg-xZn**	**MEM + 10%FBS**	**CCC**	**2.3**	**100%/day**	**1, 2, 4 d**	–	[101]
Semi static	**Pure Mg**	**DMEM Glutamax + 10% FBS**	**CCC**	**Not reported**	**100%/2–3 days**	**40 d**	–	[102]
Dynamic	AZ31	SBF	AC, 37 °C	0.79 cm^2/mL	–	10 min, 2 h	0.88 Pa	[103]
Dynamic	Pure Mg, WE43	HBSS	AC, 37 °C	1780–1666	–	240 h	0.64 Pa	[104]
Dynamic	**Mg-Zn-Ca, AZ31**	**DMEM + 10%FBS + 1% P/S**	**CCC**	**2222**	**recirculation**	**7 days**	**0, 0.07, 0.15, 0.31, 0.62 Pa**	[105]
Dynamic	Pure Mg, AZ91, ZE41	HBSS	pH and CO_2 controlled	514–654	recirculation	166 h	n/a	[106]
Dynamic/stirring	Pure Mg	PBS and HBSS	AC, 37 °C	80	stirring	120 s	Rotatory disc	[107]
Dynamic	Pure Mg	SBF	AC, 37 °C	110–132	recirculation	1, 2, 3 d	0.025, 0.4, 0.8 mL/min	[108]

Table 3
Available *in vitro* recommendations observing the V/A ratio to apply.

	DIN EN ISO 10993-12 (2007) Biological evaluation of medical devices - Part 12: Sample preparation and reference materials
Volume/area (mL/cm^2) ± 10%	0.17–0.8 (depending on the shape)
Volume/mass (mL/g) ± 10%	5–10 (depending on the shape)
	ASTM G31-72 (2004) Standard Practice for Laboratory Immersion Corrosion Testing of Metals
Volume/area (mL/cm^2)	20–40

V/A ratio proposed by both standards (Table 3) indicates the necessity to standardise the *in vitro* set-up and also explains some geographic differences. Besides, the ASTM standard points out the importance of the V/A ratio and the immersion time in order to prevent or consider possible distortions of the test conditions.

Some authors have proven the influence of the V/A ratio on the degradation rate under static conditions [5,111], revealing a limit on the ratio above which the degradation rate is independent of the V/A ratio [112], that is also shown in Fig. 6 (A). This has been explained by the limited capacity to absorb the change in pH generated by the magnesium cathodic reaction [106,113]. This effect is depicted in Fig. 6 (B), where the amount of OH^- in the medium calculated over the immersion time at different V/A ratios shows the influence of the volume in the OH^- released.

The alkalinization of the surface environment promotes a decrease in the solubility of compounds that will conform the degradation layer under simulated physiological solutions (e.g. $Mg(OH)_2$ [112], $MgCO_3$ [114,115], $CaCO_3$ [116,117], $Mg_3(PO4)_2$ or $Ca_5(PO4)_3(OH)$ [118,119]). This decrease in solubility causes the precipitation of oversaturated substances as degradation layer, which in turn is responsible for the passivation of the magnesium surface under alkaline conditions. This alkalinization process should be considered even for buffered degradation mediums when a low V/A ratio is applied [68]. Due to the static conditions limitations on the diffusion of OH^- and buffering species are induced that take place on the surface [120,121] and the dependence of the buffer capacity on the volume of the buffer [122]. For the above-mentioned reasons, the selected V/A ratio applied in static *in vitro* tests should be reported to facilitate the comparison between experiments. According to the ASTM G31-72 standard and the literature reviewed in Table 2, the selected V/A ratio should be high enough to avoid the alkalinization of the medium for the immersion time proposed as shown in Fig. 6 (A).

The implementation of the buffering system provided by cell culture conditions (CO_2/HCO_3^-) and the so-called *semi-static* methodology applied by previous authors [98] to mimic the fluid exchange in the implantation site will lead to more comparable results due to less influence of the set-up methodology (pH and concentration variation).

3.2. Dynamic conditions

Apart of the already discussed application of physiological conditions, one other major reason for the *in vitro* and *in vivo* miscorrelation is the influence of the flow conditions [107,108,120,121,124–126]. The non-well-studied mechanisms that contribute to a general higher degradation rate under dynamic conditions are currently attributed to (I) a high V/A ratio and (II) mass transfer phenomena. Regarding point (I) - due to the more complex set-up (including a reservoir, tubing apart from the degradation chamber), the applied V/A ratio is higher than under static conditions. As discussed above, this leads to a higher buffer capacity and lower possibilities to reach a saturation or depletion of relevant components. Under dynamic conditions, the degradation medium volume enclosed in the testing chamber/cell has much lower relevance than observed under static conditions. The total volume circulated through the testing chamber and the possibility of recirculating fresh medium become more relevant to achieve a reproducible environment (Fig. 7).

(II) Due to the application of flow, the convective component increases, which is under static conditions only induced by the H_2 evolution. The flow reduces the layer thickness, and the kinetics of the electrochemical process (cathodic and anodic reaction) is promoted due to a faster mass transfer in the interface between the surface and the bulk medium. However, there is a relative consensus that the applied flow rate is not enough to describe the hydrodynamic conditions surrounding the sample. The design of the testing chamber/cell translates the flow rate applied by the pumping system into a specific hydrodynamic pressure representative of the mass transfer processes on the material surface. To measure this hydrodynamic pressure, current authors have been concurred into analysing the flow-Induced shear stress (FISS) generated by the flow into the testing chamber. This hydrodynamic pressure increases the degradation rate when dynamic conditions are applied compared to static conditions at equal V/A ratios [124]. However, the degradation layer and the degradation morphology is also affected by the dynamic conditions. The changes in the mass transfer can (I) affect the kinetics of CaPs precipitation by changing the concentration of Mg^{2+} at the local surface [104], (II) modify the local chloride ion concentration, (III) generate a drag or peel-off effect on the degradation layer and (IV) modulate the local pH on the material surface by an increase of the FISS [104,121,126].

In summary, to be able to compare results and gain more insight into the mechanisms of flow influence, dynamic immersion set-ups should be defined by the following parameters:

- V/A ratio (in the whole system)
- Kind of flow (intermittent or continuous)
- Flow rate (correlated with the FISS generated)
- Chamber design and FISS generated on the surface of the material
- Flow regime. As the Reynold number presented in most of the physiological fluids are moderate (below 1000), laminar flow is assumed when computational methods are applied [128].

4. Why and what can be measured? Reliable and predictive measurements or not?

The highly simplified general degradation process shown in Fig. 8. Degradation of Mg releases ions and products into the medium used which in turn generates a mass loss of the sample. On the other hand, the environment on the interface sample/degradation medium (pH, temperature and concentrations) promote the degradation layer build up by the combination of species derived from the medium (e.g. Mg^{2+}, Ca^{2+}, HCO_3^- and the alloy (Mg^{2+} and alloying elements)).

4.1. Determination of degradation rate

Mass loss measurements are the simplest form of evaluation available for degrading materials. Mass loss of the immersed sample is used to determine its degradation rate using ASTM standard [109]. Here again, the results obtained may vary as the degradation is influenced by the simulated medium employed. The degradation products developed on the surface are crucial to controlling the degradation kinetics. Chromic acid treatment (180 g/L in distilled water) facilitates the removal of the degradation layer providing an opportunity to visualise the degraded surface

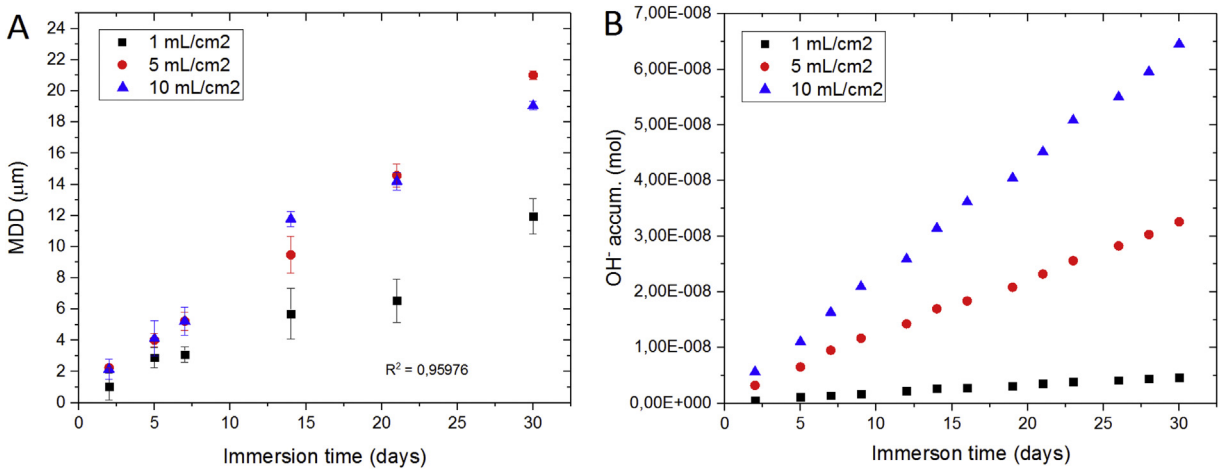

Fig. 6. A) Mean degradation depth (MDD) on Mg-2Ag over 30 days of immersion under cell culture conditions (37 °C, 20% O2, 5% CO2, 95% rH) in α-MEM with the addition of 10% FBS and 1% P/S for different at different V/A ratios. MDD values on this graph were calculated based on reference [123]. B) Amount of OH^- ions calculated from the pH measured for the different V/A ratio applied.

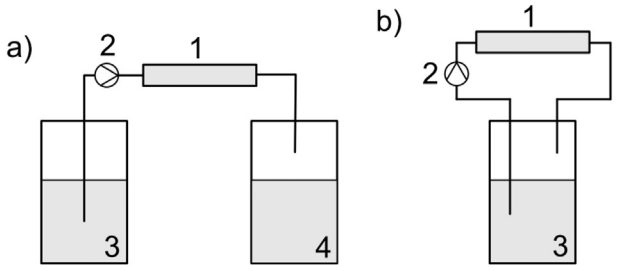

Fig. 7. Dynamic operation set-ups design considering a) constant fresh medium circulation, and b) recirculation of the medium. Adapted from Ref. [127]. (1) Testing chamber, (2) pumping system, (3) medium reservoir, (4) waist medium reservoir.

morphology [129]. In case of porosity and sub-surface cracks that appear in the layer, it is possible that Cl^- aggregates might remain within the layer. During the chromic acid treatment, these aggregates may react with chromic acid and water causing further degradation that is not desirable in the final stages [130]. Hence, compounds like silver nitrate ($AgNO_3$; 2 g/L in distilled water) is added to chromic acid to reduce these deleterious effects. Most of the alloying elements are inert in contact chromic acid, however certain elements like silicone, zirconium and others may interact with chromates [131,132]. Therefore, it is of importance to check

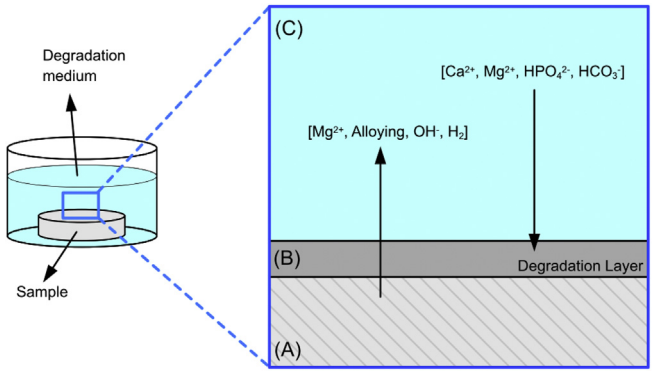

Fig. 8. General material flow concerning Mg degradation under physiological conditions.

magnesium alloys for interaction prior to chromic acid treatment. Also, if e.g. Ag containing Mg alloys are analysed, the addition of $AgNO_3$ should be avoided. Another gravimetric method to determine the degradation rate is the hydrogen generation or eudiometric method [133]. As under physiological conditions, experiments are performed either in a gaseous atmosphere in the incubator [90], or by gassing of the medium [106]. However, not many studies have been conducted with eudiometric setups. A general concern about the validity of this determination of mass loss/degradation rate should be stated, as (I) magnesium degradation influences directly the amount of O_2 and CO_2 in solution [99] and (II) many ingredients of physiological solutions have hydrogen-binding capacities including the medium buffering systems as stated before. Therefore, if such methods are used, the nature of the escaped gas should be either validated by e.g. gas chromatography [134], or the use of sophisticated sensors for hydrogen is proposed [135].

4.2. pH and ion concentration

The formation of hydroxide layer during initial degradation is generally accompanied by a transient increase in pH [67] as exposed in Equation (3). The hydroxide layer is thermodynamically stable at pH-values higher than 8.3. This assumes a decrease in degradation rate over time as the layer is attaining stability. However, the presence of Cl^- ions promotes the formation of water-soluble $MgCl_2$ from the layer, then making degradation continuing. pH implicitly cannot be a good indicator under physiological conditions as it changes rather quickly between measurement times. This can lead to misinterpretation of the data [112]. Nevertheless, studies on the influence of pH on degradation is of interest because of the variance in the formed products with different pH levels in the buffered medium [106,136,137]. The degradation rate decreases in basic pH regimes compared to the acidic solutions. This is mainly attributed to the formation of stable hydroxide layer in the adopted solutions. In many *in vitro* studies pH is maintained constant to understand the influence of physiological conditions on degradation (e.g. Ref. [138]).

Detection methods like Flame AAS and ICP mass spectrometry were employed to monitor the release of Mg and other metal ions in the cell culture medium during degradation [139,140]. Studies on metal ions release in ZK30 and WE-type Mg alloys with ICP-OES revealed the increase in Mg ions with a simultaneous drop in Ca

and P ions release during initial stages of immersion. Zn and Zr concentrations measured were below 0.001 mmol/L in these studies [141]. Experiments related to coatings on pure Mg samples using ICP-AES showed a huge increase in Mg ion release compared to non-coated pure Mg samples [142] in the extract.

As evident and reliable the ion release technique for inferring Mg degradation appears, the technique has its difficulties when it comes to complex solutions or even tissue analysis. The elemental standards for these chemical methods are not directly transferable [143]. Often, the presence of other metal ions existing in the sample solutions interfere with the element of detection. Improper matrix preparation or the choice of element-specific wavelengths in AAS can be among the multiple reasons that lead to this ambiguity. With respect to this, it is important to develop an appropriate matrix standard method [144].

Osmolality measurements can also provide information about the amount of released substances into the fluid [145] and is expected to be directly correlated with the degradation rate of the alloy. Willumeit-Römer et al. [146] reported that the osmolality increased even in the presence of medium containing protein complex. The weakest increase in osmolality over time was reported in deionized water, demonstrating again the influence of the pH and the buffering system on the degradation process revealed in this case by differences on the amount of released substances.

5. Conclusion

The analysis of magnesium degradation has made a big step forward over the last decade leading to models predicting the *in vivo* degradation rate. However, the mechanisms are still far from full understanding and more effort should be taken to determine these. To reach this goal, the application of physiological conditions still seems to be a basic requirement. Additionally, such setups should also be applied in other fields dealing with degrading materials.

Conflicts of interest

The authors declare no conflict of interest.

Acknowledgment

We would like to thank the China Scholarship Council (CSC) for a scholarship to RQH. The research leading to these results has received funding from the Helmholtz Virtual Institute "*In vivo* studies of biodegradable magnesium based implant materials (MetBioMat)" under grant agreement n° VH-VI-523.

References

[1] B.J.C. Luthringer, F. Feyerabend, R. Willumeit-Römer, Magnesium-based implants: a mini review, Magnes. Res. 27 (4) (2014) 142–154.
[2] M. Kieke, F. Feyerabend, J. Lemaitre, P. Behrens, R. Willumeit-Römer, Degradation rates and products of pure magnesium exposed to different aqueous media under physiological conditions, BioNanoMaterials (2016) 131–143.
[3] D. Tie, F. Feyerabend, N. Hort, R. Willumeit, D. Hoeche, XPS studies of magnesium surfaces after exposure to Dulbecco's modified eagle medium, Hank's buffered salt solution, and simulated body fluid, Adv. Eng. Mater. 12 (12) (2010) B699–B704.
[4] M. Bohner, J. Lemaitre, Can bioactivity be tested in vitro with SBF solution? Biomaterials 30 (12) (2009) 2175–2179.
[5] L. Yang, E. Zhang, Biocorrosion behavior of magnesium alloy in different simulated fluids for biomedical application, Mater. Sci. Eng. C 29 (5) (2009) 1691–1696.
[6] R. Rettig, S. Virtanen, Composition of corrosion layers on a magnesium rare-earth alloy in simulated body fluids, J. Biomed. Mater. Res. Part A 88 (2) (2009) 359–369.
[7] A. Yamamoto, S. Hiromoto, Effect of inorganic salts, amino acids and proteins on the degradation of pure magnesium in vitro, Mater. Sci. Eng. C 29 (5) (2009) 1559–1568.
[8] M. Esmaily, J.E. Svensson, S. Fajardo, N. Birbilis, G.S. Frankel, S. Virtanen, R. Arrabal, S. Thomas, L.G. Johansson, Fundamentals and advances in magnesium alloy corrosion, Prog. Mater. Sci. 89 (2017) 92–193.
[9] B. Hadzima, M. Mhaede, F. Pastorek, Electrochemical characteristics of calcium-phosphatized AZ31 magnesium alloy in 0.9% NaCl solution, J. Mater. Sci. Mater. Med. 25 (5) (2014) 1227–1237.
[10] D. Zhao, T. Wang, X. Guo, J. Kuhlmann, A. Doepke, Z. Dong, V.N. Shanov, W.R. Heineman, Monitoring biodegradation of magnesium implants with sensors, JOM 68 (4) (2016) 1204–1208.
[11] L. Yang, N. Hort, R. Willumeit, F. Feyerabend, Effects of corrosion environment and proteins on magnesium corrosion, Corros. Eng. Sci. Technol. 47 (5) (2012) 335–339.
[12] T. Kokubo, H. Takadama, How useful is SBF in predicting in vivo bone bioactivity? Biomaterials 27 (15) (2006) 2907–2915.
[13] A. Oyane, H.M. Kim, T. Furuya, T. Kokubo, T. Miyazaki, T. Nakamura, Preparation and assessment of revised simulated body fluids, J. Biomed. Mater. Res. Part A 65 (2) (2003) 188–195.
[14] M.P. Staiger, F. Feyerabend, R. Willumeit, C.S. Sfeir, Y.F. Zheng, S. Virtanen, W.D. Müeller, A. Atrens, M. Peuster, P.N. Kumta, D. Mantovani, F. Witte, Summary of the panel discussions at the 2nd symposium on biodegradable metals, Maratea, Italy, 2010, Mater. Sci. Eng. B 176 (20) (2011) 1596–1599.
[15] N.A. Agha, F. Feyerabend, B. Mihailova, S. Heidrich, U. Bismayer, R. Willumeit-Romer, Magnesium degradation influenced by buffering salts in concentrations typical of in vitro and in vivo models, Mater. Sci. Eng. C Mater. Biol. Appl. 58 (2016) 817–825.
[16] Y. Xin, P.K. Chu, Influence of Tris in simulated body fluid on degradation behavior of pure magnesium, Mater. Chem. Phys. 124 (1) (2010) 33–35.
[17] R. Walter, M.B. Kannan, In-vitro degradation behaviour of WE54 magnesium alloy in simulated body fluid, Mater. Lett. 65 (4) (2011) 748–750.
[18] M. Schinhammer, J. Hofstetter, C. Wegmann, F. Moszner, J.F. Löffler, P.J. Uggowitzer, On the immersion testing of degradable implant materials in simulated body fluid: active pH regulation using CO_2, Adv. Eng. Mater. 15 (6) (2013) 434–441.
[19] Y. Xin, T. Hu, P.K. Chu, Degradation behaviour of pure magnesium in simulated body fluids with different concentrations of HCO3-, Corros. Sci. 53 (4) (2011) 1522–1528.
[20] A.C. Hänzi, I. Gerber, M. Schinhammer, J.F. Löffler, P.J. Uggowitzer, On the in vitro and in vivo degradation performance and biological response of new biodegradable Mg–Y–Zn alloys, Acta Biomater. 6 (5) (2010) 1824–1833.
[21] N.I.Z. Abidin, A.D. Atrens, D. Martin, A. Atrens, Corrosion of high purity Mg, Mg2Zn0. 2Mn, ZE41 and AZ91 in Hank's solution at 37 C, Corros. Sci. 53 (11) (2011) 3542–3556.
[22] P. Shi, W.F. Ng, M.H. Wong, F.T. Cheng, Improvement of corrosion resistance of pure magnesium in Hanks' solution by microarc oxidation with sol–gel TiO2 sealing, J. Alloys Compd. 469 (1) (2009) 286–292.
[23] S. Johnston, Z. Shi, A. Atrens, The influence of pH on the corrosion rate of high-purity Mg, AZ91 and ZE41 in bicarbonate buffered Hanks' solution, Corros. Sci. 101 (2015) 182–192.
[24] N.I.Z. Abidin, B. Rolfe, H. Owen, J. Malisano, D. Martin, J. Hofstetter, P.J. Uggowitzer, A. Atrens, The in vivo and in vitro corrosion of high-purity magnesium and magnesium alloys WZ21 and AZ91, Corros. Sci. 75 (2013) 354–366.
[25] N.T. Kirkland, J. Waterman, N. Birbilis, G. Dias, T.B. Woodfield, R.M. Hartshorn, M.P. Staiger, Buffer-regulated biocorrosion of pure magnesium, J. Mater. Sci. Mater. Med. 23 (2) (2012) 283–291.
[26] I. Marco, A. Myrissa, E. Martinelli, F. Feyerabend, R. Willumeit-Römer, A. Weinberg, O. Van der Biest, In vivo and in vitro degradation comparison of pure Mg, Mg-10Gd and Mg-2Ag: a short term study, Eur. Cells Mater. 33 (2017) 90–104.
[27] I. Johnson, D. Perchy, H. Liu, In vitro evaluation of the surface effects on magnesium-yttrium alloy degradation and mesenchymal stem cell adhesion, J. Biomed. Mater. Res. A 100 (2) (2012) 477–485.
[28] F. Feyerabend, H. Drucker, D. Laipple, C. Vogt, M. Stekker, N. Hort, R. Willumeit, Ion release from magnesium materials in physiological solutions under different oxygen tensions, J. Mater. Sci. Mater. Med. 23 (1) (2012) 9–24.
[29] X.B. Chen, D.R. Nisbet, R.W. Li, P.N. Smith, T.B. Abbott, M.A. Easton, D.H. Zhang, N. Birbilis, Controlling initial biodegradation of magnesium by a biocompatible strontium phosphate conversion coating, Acta Biomater. 10 (3) (2014) 1463–1474.
[30] N. Kirkland, J. Lespagnol, N. Birbilis, M. Staiger, A survey of bio-corrosion rates of magnesium alloys, Corros. Sci. 52 (2) (2010) 287–291.
[31] I. Marco, F. Feyerabend, R. Willumeit-Römer, O. Van der Biest, Influence of testing environment on the degradation behavior of magnesium alloys for bioabsorbable implants, in: TMS 2015, 144th Annual Meeting & Exhibition, John Wiley & Sons, Inc, 2015, pp. 497–506.
[32] N.E. Good, G.D. Winget, W. Winter, T.N. Connolly, S. Izawa, R.M.M. Singh, Hydrogen ion buffers for biological research, Biochemistry 5 (2) (1966) 467–477.
[33] C. Schille, M. Braun, H.P. Wendel, L. Scheideler, N. Hort, H.P. Reichel, E. Schweizer, J. Geis-Gerstorfer, Corrosion of experimental magnesium alloys in blood and PBS: a gravimetric and microscopic evaluation, Mater. Sci. Eng. B 176 (20) (2011) 1797–1801.

[34] S. Naddaf Dezfuli, Z. Huan, J.M.C. Mol, M.A. Leeflang, J. Chang, J. Zhou, Influence of HEPES buffer on the local pH and formation of surface layer during in vitro degradation tests of magnesium in DMEM, Prog. Nat. Sci. Mater. Int. 24 (5) (2014) 531–538.

[35] J. Walker, S. Shadanbaz, N.T. Kirkland, E. Stace, T. Woodfield, M.P. Staiger, G.J. Dias, Magnesium alloys: predicting in vivo corrosion with in vitro immersion testing, J. Biomed. Mater. Res. Part B Appl. Biomater. 100 (4) (2012) 1134–1141.

[36] M.B. Kannan, H. Khakbaz, A. Yamamoto, Understanding the influence of HEPES buffer concentration on the biodegradation of pure magnesium: an electrochemical study, Mater. Chem. Phys. 197 (2017) 47–56.

[37] K. Törne, A. Örnberg, J. Weissenrieder, The influence of buffer system and biological fluids on the degradation of magnesium, J. Biomed. Mater. Res. Part B Appl. Biomater. 105 (6) (2017) 1490–1502.

[38] D. Rohanova, D. Horkavcova, L. Paidere, A.R. Boccaccini, P. Bozdechova, P. Bezdicka, Interaction of HEPES buffer with glass-ceramic scaffold: can HEPES replace TRIS in SBF? J. Biomed. Mater. Res. Part B Appl. Biomater. 106 (1) (2018) 143–152.

[39] Y. Xin, T. Hu, P.K. Chu, Influence of test solutions on in vitro studies of biomedical magnesium alloys, J. Electrochem. Soc. 157 (7) (2010) C238.

[40] L.-Y. Cui, Y. Hu, R.-C. Zeng, Y.-X. Yang, D.-D. Sun, S.-Q. Li, F. Zhang, E.-H. Han, New insights into the effect of Tris-HCl and Tris on corrosion of magnesium alloy in presence of bicarbonate, sulfate, hydrogen phosphate and dihydrogen phosphate ions, J. Mater. Sci. Technol. 33 (9) (2017) 971–986.

[41] R. Lindström, L.-G. Johansson, G.E. Thompson, P. Skeldon, J.-E. Svensson, Corrosion of magnesium in humid air, Corros. Sci. 46 (5) (2004) 1141–1158.

[42] Y. Xin, T. Hu, P.K. Chu, Degradation behaviour of pure magnesium in simulated body fluids with different concentrations of HCO3, Corros. Sci. 53 (4) (2011) 1522–1528.

[43] Z. Li, G.-L. Song, S. Song, Effect of bicarbonate on biodegradation behaviour of pure magnesium in a simulated body fluid, Electrochim. Acta 115 (Supplement C) (2014) 56–65.

[44] G. Gstraunthaler, T. Lindl, Zell- und Gewebkultur, Springer Spektrum, 2013.

[45] F. Astrup, O.S. Andersen, K. Jorgensen, K. Engel, The acid-base metabolism, The Lancet 275(7133) 1035–1039.

[46] Y. Xin, K. Huo, H. Tao, G. Tang, P.K. Chu, Influence of aggressive ions on the degradation behavior of biomedical magnesium alloy in physiological environment, Acta Biomater. 4 (6) (2008) 2008–2015.

[47] N.A. Agha, F. Feyerabend, B. Mihailova, S. Heidrich, U. Bismayer, R. Willumeit-Römer, Magnesium degradation influenced by buffering salts in concentrations typical of in vitro and in vivo models, Mater. Sci. Eng. C 58 (Supplement C) (2016) 817–825.

[48] L. Xu, E. Zhang, D. Yin, S. Zeng, K. Yang, In vitro corrosion behaviour of Mg alloys in a phosphate buffered solution for bone implant application, J. Mater. Sci. Mater. Med. 19 (3) (2008) 1017–1025.

[49] G. Ellison, J.V. Straumfjord, J. Hummel, Buffer capacities of human blood and plasma, Clin. Chem. 4 (6) (1958) 452–461.

[50] V. Wagener, S. Virtanen, Protective layer formation on magnesium in cell culture medium, Mater. Sci. Eng. C 63 (2016) 341–351.

[51] X. Gu, Y. Zheng, L. Chen, Influence of artificial biological fluid composition on the biocorrosion of potential orthopedic Mg–Ca, AZ31, AZ91 alloys, Biomed. Mater. 4 (6) (2009), 065011.

[52] C.L. Liu, Y.J. Wang, R.C. Zeng, X.M. Zhang, W.J. Huang, P.K. Chu, In vitro corrosion degradation behaviour of Mg–Ca alloy in the presence of albumin, Corros. Sci. 52 (10) (2010) 3341–3347.

[53] D. Hoche, C. Blawert, S.V. Lamaka, N. Scharnagl, C. Mendis, M.L. Zheludkevich, The effect of iron re-deposition on the corrosion of impurity-containing magnesium, Phys. Chem. Chem. Phys. 18 (2) (2016) 1279–1291.

[54] S.V. Lamaka, D. Höche, R.P. Petrauskas, C. Blawert, M.L. Zheludkevich, A new concept for corrosion inhibition of magnesium: suppression of iron redeposition, Electrochem. Commun. 62 (Supplement C) (2016) 5–8.

[55] J.N. Adkins, S.M. Varnum, K.J. Auberry, R.J. Moore, N.H. Angell, R.D. Smith, D.L. Springer, J.G. Pounds, Toward a human blood serum proteome: analysis by multidimensional separation coupled with mass spectrometry, Mol. Cell. Proteomics 1 (12) (2002) 947–955.

[56] A. Loban, R. Kime, H. Powers, Iron-binding antioxidant potential of plasma albumin, Clin. Sci. 93 (5) (1997) 445–451.

[57] I. Kasvosve, J. Delanghe, Total iron binding capacity and transferrin concentration in the assessment of iron status, Clin. Chem. Lab. Med. (2002) 1014.

[58] R.F. Ritchie, G.E. Palomaki, L.M. Neveux, O. Navolotskaia, T.B. Ledue, W.Y. Craig, Reference distributions for the negative acute-phase serum proteins, albumin, transferrin and transthyretin: a practical, simple and clinically relevant approach in a large cohort, J. Clin. Lab. Anal. 13 (6) (1999) 273–279.

[59] A.S. Borges, T.J. Divers, T. Stokol, O.H. Mohammed, Serum iron and plasma fibrinogen concentrations as indicators of systemic inflammatory diseases in horses, J. Vet. Intern. Med. 21 (3) (2007) 489–494.

[60] K. Orino, Functional binding analysis of human fibrinogen as an iron- and heme-binding protein, BioMetals 26 (5) (2013) 789–794.

[61] A.H. Martinez Sanchez, B.J. Luthringer, F. Feyerabend, R. Willumeit, Mg and Mg alloys: how comparable are in vitro and in vivo corrosion rates? A review, Acta Biomater. 13 (2015) 16–31.

[62] F. Witte, N. Hort, C. Vogt, S. Cohen, R. Willumeit, K.U. Kainer, F. Feyerabend, Degradable biomaterials based on magnesium corrosion, Curr. Opin. Solid State Mater. Sci. 12 (2008) 63–72.

[63] N.T. Kirkland, N. Birbilis, J. Walker, T. Woodfield, G.J. Dias, M.P. Staiger, In-vitro dissolution of magnesium–calcium binary alloys: clarifying the unique role of calcium additions in bioresorbable magnesium implant alloys, J. Biomed. Mater. Res. Part B Appl. Biomater. 95 (1) (2010) 91–100.

[64] J. Zhang, N. Kong, Y.J. Shi, J.L. Niu, L. Mao, H.Y. Li, M.P. Xiong, G.Y. Yuan, Influence of proteins and cells on in vitro corrosion of Mg-Nd-Zn-Zr alloy, Corros. Sci. 85 (2014) 477–481.

[65] E. Mouzou, C. Paternoster, R. Tolouei, P. Chevallier, C.A. Biffi, A. Tuissi, D. Mantovani, CO2-rich atmosphere strongly affects the degradation of Fe-21Mn-1C for biodegradable metallic implants, Mater. Lett. 181 (2016) 362–366.

[66] N.A. Agha, F. Feyerabend, B. Mihailova, S. Heidrich, U. Bismayer, R. Willumeit-Römer, Magnesium degradation influenced by buffering salts in concentrations typical of in vitro and in vivo models, Mater. Sci. Eng. C 58 (2016) 817–825.

[67] N. Ahmad Agha, R. Willumeit-Romer, D. Laipple, B. Luthringer, F. Feyerabend, The degradation interface of magnesium based alloys in direct contact with human primary osteoblast cells, PLoS One 11 (6) (2016), e0157874.

[68] S. Virtanen, Biodegradable Mg and Mg alloys: corrosion and biocompatibility, Mater. Sci. Eng. B 176 (20) (2011) 1600–1608.

[69] R. Willumeit, F. Feyerabend, N. Huber, Magnesium degradation as determined by artificial neural networks, Acta Biomater. 9 (10) (2013) 8722–8729.

[70] R. Willumeit, J. Fischer, F. Feyerabend, N. Hort, U. Bismayer, S. Heidrich, B. Mihailova, Chemical surface alteration of biodegradable magnesium exposed to corrosion media, Acta Biomater. 7 (6) (2011) 2704–2715.

[71] Y.F. Zheng, X.N. Gu, Y.L. Xi, D.L. Chai, In vitro degradation and cytotoxicity of Mg/Ca composites produced by powder metallurgy, Acta Biomater. 6 (5) (2010) 1783–1791.

[72] N. Erdmann, N. Angrisani, J. Reifenrath, A. Lucas, F. Thorey, D. Bormann, A. Meyer-Lindenberg, Biomechanical testing and degradation analysis of MgCa0.8 alloy screws: a comparative in vivo study in rabbits, Acta Biomater. 7 (3) (2011) 1421–1428.

[73] C. Rossig, N. Angrisani, P. Helmecke, S. Besdo, J.M. Seitz, B. Welke, N. Fedchenko, H. Kock, J. Reifenrath, In vivo evaluation of a magnesium-based degradable intramedullary nailing system in a sheep model, Acta Biomater. 25 (2015) 369–383.

[74] J.H. Nordlien, S. Ono, N. Masuko, K. Nisancioglu, A TEM investigation of naturally formed oxide films on pure magnesium, Corros. Sci. 39 (8) (1997) 1397–1414.

[75] O. Jung, R. Smeets, D. Porchetta, A. Kopp, C. Ptock, U. Müller, M. Heiland, M. Schwade, B. Behr, N. Kröger, L. Kluwe, H. Hanken, P. Hartjen, Optimized in vitro procedure for assessing the cytocompatibility of magnesium-based biomaterials, Acta Biomater. 23 (2015) 354–363.

[76] J. Wang, F. Witte, T. Xi, Y. Zheng, K. Yang, Y. Yang, D. Zhao, J. Meng, Y. Li, W. Li, K. Chan, L. Qin, Recommendation for modifying current cytotoxicity testing standards for biodegradable magnesium-based materials, Acta Biomater. 21 (Supplement C) (2015) 237–249.

[77] A.J. Bard, L.R. Faulkner, in: Electrochemical Methods: Fundamentals and Applications, second ed., John Wiley & Sons, 2001.

[78] X.N. Gu, et al., Influence of artificial biological fluid composition on the biocorrosion of potential orthopedic Mg-Ca, AZ31, AZ91 alloys, Biomed. Mater. 4 (6) (2009), 065011.

[79] C. Lorenz, J.G. Brunner, P. Kollmannsberger, L. Jaafar, B. Fabry, S. Virtanen, Effect of surface pre-treatments on biocompatibility of magnesium, Acta Biomater. 5 (7) (2009) 2783–2789.

[80] C.L. Liu, Y.J. Wang, R.C. Zeng, X.M. Zhang, W.J. Huang, P.K. Chu, In vitro corrosion degradation behaviour of Mg-Ca alloy in the presence of albumin, Corros. Sci. 52 (10) (2010) 3341–3347.

[81] N.T. Kirkland, N. Birbilis, J. Walker, T. Woodfield, G.J. Dias, M.P. Staiger, In-vitro dissolution of magnesium–calcium binary alloys: clarifying the unique role of calcium additions in bioresorbable magnesium implant alloys, J. Biomed. Mater. Res. Part B Appl. Biomater. 95B (1) (2010) 91–100.

[82] J.A. Grogan, S.B. Leen, P.E. McHugh, A physical corrosion model for bioabsorbable metal stents, Acta Biomater. 10 (5) (2014) 2313–2322.

[83] Y. Wang, C.S. Lim, C.V. Lim, M.S. Yong, E.K. Teo, L.N. Moh, In vitro degradation behavior of M1A magnesium alloy in protein-containing simulated body fluid, Mater. Sci. Eng. C 31 (3) (2011) 579–587.

[84] P.K. Bowen, J. Drelich, J. Goldman, A new in vitro–in vivo correlation for bioabsorbable magnesium stents from mechanical behavior, Mater. Sci. Eng. C 33 (8) (2013) 5064–5070.

[85] A. Samaniego, K. Gusieva, I. Llorente, S. Feliu Jr., N. Birbilis, Exploring the possibility of protective surface oxides upon Mg alloy AZ31 via lutetium additions, Corros. Sci. 89 (2014) 101–110.

[86] R.-C. Zeng, X.-T. Li, L.-J. Liu, S.-Q. Li, F. Zhang, In vitro degradation of pure Mg for esophageal stent in artificial saliva, J. Mater. Sci. Technol. 32 (5) (2016) 437–444.

[87] E. Matykina, I. Garcia, R. Arrabal, M. Mohedano, B. Mingo, J. Sancho, M.C. Merino, A. Pardo, Role of PEO coatings in long-term biodegradation of a Mg alloy, Appl. Surf. Sci. 389 (2016) 810–823.

[88] R.-C. Zeng, X.-T. Li, S.-Q. Li, F. Zhang, E.-H. Han, In vitro degradation of pure Mg in response to glucose, Sci. Rep. 5 (2015) 13026.

[89] S. Hiromoto, M. Inoue, T. Taguchi, M. Yamane, N. Ohtsu, In vitro and in vivo

biocompatibility and corrosion behaviour of a bioabsorbable magnesium alloy coated with octacalcium phosphate and hydroxyapatite, Acta Biomater. 11 (Supplement C) (2015) 520–530.
[90] I. Marco, F. Feyerabend, R. Willumeit-Römer, O. Van der Biest, Influence of testing environment on the degradation behavior of magnesium alloys for bioabsorbable implants, in: TMS 2015 144th Annual Meeting & Exhibition: Supplemental Proceedings, Springer International Publishing, Cham, 2016, pp. 499–506.
[91] I. Marco, F. Feyerabend, R. Willumeit-Römer, O. Van der Biest, Degradation testing of Mg alloys in Dulbecco's modified eagle medium: influence of medium sterilization, Mater. Sci. Eng. C 62 (2016) 68–78.
[92] W. Jin, G. Wu, A. Gao, H. Feng, X. Peng, P.K. Chu, Hafnium-implanted WE43 magnesium alloy for enhanced corrosion protection and biocompatibility, Surf. Coat. Technol. 306 (Part A) (2016) 11–15.
[93] L. Hou, Z. Li, H. Zhao, Y. Pan, S. Pavlinich, X. Liu, X. Li, Y. Zheng, L. Li, Microstructure, mechanical properties, corrosion behavior and biocompatibility of as-extruded biodegradable Mg–3Sn–1Zn–0.5Mn alloy, J. Mater. Sci. Technol. 32 (9) (2016) 874–882.
[94] Y. Wang, L.-Y. Cui, R.-C. Zeng, S.-Q. Li, Y.-H. Zou, E.-H. Han, In vitro degradation of pure magnesium—the effects of glucose and/or amino acid, Materials 10 (7) (2017) 725.
[95] E. Galvin, S. Jaiswal, C. Lally, B. MacDonald, B. Duffy, In vitro corrosion and biological assessment of bioabsorbable WE43 Mg alloy specimens, J. Manuf. Mater. Process. 1 (1) (2017) 8.
[96] A.C. Hänzi, P. Gunde, M. Schinhammer, P.J. Uggowitzer, On the biodegradation performance of an Mg–Y–RE alloy with various surface conditions in simulated body fluid, Acta Biomater. 5 (1) (2009) 162–171.
[97] X. Zhang, Z. Wang, G. Yuan, Y. Xue, Improvement of mechanical properties and corrosion resistance of biodegradable Mg–Nd–Zn–Zr alloys by double extrusion, Mater. Sci. Eng. B 177 (13) (2012) 1113–1119.
[98] J. Walker, S. Shadanbaz, N.T. Kirkland, E. Stace, T. Woodfield, M.P. Staiger, G.J. Dias, Magnesium alloys: predicting in vivo corrosion with in vitro immersion testing, J. Biomed. Mater. Res. Part B Appl. Biomater. 100B (4) (2012) 1134–1141.
[99] F. Feyerabend, H. Drücker, D. Laipple, C. Vogt, M. Stekker, N. Hort, R. Willumeit, Ion release from magnesium materials in physiological solutions under different oxygen tensions, J. Mater. Sci. Mater. Med. 23 (1) (2012) 9–24.
[100] Y. Jang, B. Collins, J. Sankar, Y. Yun, Effect of biologically relevant ions on the corrosion products formed on alloy AZ31B: an improved understanding of magnesium corrosion, Acta Biomater. 9 (10) (2013) 8761–8770.
[101] J. Walker, S. Shadanbaz, T.B.F. Woodfield, M.P. Staiger, G.J. Dias, The in vitro and in vivo evaluation of the biocompatibility of Mg alloys, Biomed. Mater. 9 (1) (2014), 015006.
[102] M. Dahms, D. Höche, N. Ahmad Agha, F. Feyerabend, R. Willumeit-Römer, A simple model for long-time degradation of magnesium under physiological conditions, Mater. Corros. 69 (2) (2018) 191–196.
[103] Y.F. Zhang, B. Hinton, G. Wallace, X. Liu, M. Forsyth, On corrosion behaviour of magnesium alloy AZ31 in simulated body fluids and influence of ionic liquid pretreatments, Corros. Eng. Sci. Technol. 47 (5) (2012) 374–382.
[104] N. Li, C. Guo, Y.H. Wu, Y.F. Zheng, L.Q. Ruan, Comparative study on corrosion behaviour of pure Mg and WE43 alloy in static, stirring and flowing Hanks solution, Corros. Eng. Sci. Technol. 47 (5) (2012) 346–351.
[105] J. Wang, V. Giridharan, V. Shanov, Z. Xu, B. Collins, L. White, Y. Jang, J. Sankar, N. Huang, Y. Yun, Flow-induced corrosion behavior of absorbable magnesium-based stents, Acta Biomater. 10 (12) (2014) 5213–5223.
[106] S. Johnston, Z. Shi, A. Atrens, The influence of pH on the corrosion rate of high-purity Mg, AZ91 and ZE41 in bicarbonate buffered Hanks' solution, Corros. Sci. 101 (Supplement C) (2015) 182–192.
[107] I. Marco, O. Van der Biest, Polarization measurements from a rotating disc electrode for characterization of magnesium corrosion, Corros. Sci. 102 (2016) 384–393.
[108] A.P. Md. Saad, N. Jasmawati, M.N. Harun, M.R. Abdul Kadir, H. Nur, H. Hermawan, A. Syahrom, Dynamic degradation of porous magnesium under a simulated environment of human cancellous bone, Corros. Sci. 112 (2016) 495–506.
[109] ASTM, G31-72(2004) Standard Practice for Laboratory Immersion Corrosion Testing of Metals, ASTM International, West Conshohocken, PA, 2004, p. 8.
[110] ISO, ISO 10993-Biologische Beurteilung von Medizinprodukten, International Organisation for Standardization, 1999.
[111] K. Lips, P. Schmutz, M. Heer, P.J. Uggowitzer, S. Virtanen, Elektrochemische Korrosionsuntersuchungen an der Magnesiumlegierung AZ91: Beschreibung kritischer Parameter und deren Einfluss auf die Angriffsmechanismen auf NRC-Proben, Mater. Corros. 55 (1) (2004) 5–17.
[112] N.T. Kirkland, N. Birbilis, M.P. Staiger, Assessing the corrosion of biodegradable magnesium implants: a critical review of current methodologies and their limitations, Acta Biomater. 8 (3) (2012) 925–936.
[113] A. Dhanapal, S. Rajendraboopathy, V. Balasubramanian, S.R. Rao, A.R.T. Zaman, Effect of pH values, chloride ion concentration and exposure time on pitting corrosion rates of friction stir welded AZ61A magnesium alloy in sodium chloride solution using surface response methodology, Corros. Eng. Sci. Technol. 47 (6) (2012) 425–440.
[114] A.-H.A. Park, L.-S. Fan, CO2 mineral sequestration: physically activated dissolution of serpentine and pH swing process, Chem. Eng. Sci. 59 (22) (2004) 5241–5247.
[115] Z. Zhang, Y. Zheng, Y. Ni, Z. Liu, J. Chen, X. Liang, Temperature- and pH-dependent morphology and FT–IR analysis of magnesium carbonate hydrates, J. Phys. Chem. B 110 (26) (2006) 12969–12973.
[116] S. Stocks-Fischer, J.K. Galinat, S.S. Bang, Microbiological precipitation of CaCO3, Soil Biol. Biochem. 31 (11) (1999) 1563–1571.
[117] M.M. Tlili, M. Benamor, C. Gabrielli, H. Perrot, B. Tribollet, Influence of the interfacial pH on electrochemical CaCO3 precipitation, J. Electrochem. Soc. 150 (11) (2003) C765–C771.
[118] A. Ferreira, C. Oliveira, F. Rocha, The different phases in the precipitation of dicalcium phosphate dihydrate, J. Cryst. Growth 252 (4) (2003) 599–611.
[119] O. Mekmene, S. Quillard, T. Rouillon, J.-M. Bouler, M. Piot, F. Gaucheron, Effects of pH and Ca/P molar ratio on the quantity and crystalline structure of calcium phosphates obtained from aqueous solutions, Dairy Sci. Technol. 89 (3) (2009) 301–316.
[120] S. Hiromoto, A. Yamamoto, N. Maruyama, H. Somekawa, T. Mukai, Influence of pH and flow on the polarisation behaviour of pure magnesium in borate buffer solutions, Corros. Sci. 50 (12) (2008) 3561–3568.
[121] J. Wang, Y. Jang, G. Wan, V. Giridharan, G.-L. Song, Z. Xu, Y. Koo, P. Qi, J. Sankar, N. Huang, Y. Yun, Flow-induced corrosion of absorbable magnesium alloy: in-situ and real-time electrochemical study, Corros. Sci. 104 (2016) 277–289.
[122] N. Rodríguez-Laguna, A. Rojas-Hernández, M.T. Ramírez-Silva, R. Moya-Hernández, R. Gómez-Balderas, M.A. Romero-Romo, The conditions needed for a buffer to set the pH in a system, in: V.D. Hoang (Ed.), Advances in Titration Techniques, InTech, Rijeka, 2017 p. Ch. 01.
[123] E. Nidadavolu, F. Feyerabend, T. Ebel, R. Willumeit-Römer, M. Dahms, On the determination of magnesium degradation rates under physiological conditions, Materials 9 (8) (2016) 627.
[124] J.A. Grogan, D. Gastaldi, M. Castelletti, F. Migliavacca, G. Dubini, P.E. McHugh, A novel flow chamber for biodegradable alloy assessment in physiologically realistic environments, Rev. Sci. Instrum. 84 (9) (2013), 094301.
[125] J. Levesque, H. Hermawan, D. Dube, D. Mantovani, Design of a pseudo-physiological test bench specific to the development of biodegradable metallic biomaterials, Acta Biomater. 4 (2) (2008) 284–295.
[126] J. Wang, L. Liu, Y. Wu, M.F. Maitz, Z. Wang, Y. Koo, A. Zhao, J. Sankar, D. Kong, N. Huang, Y. Yun, Ex vivo blood vessel bioreactor for analysis of the biodegradation of magnesium stent models with and without vessel wall integration, Acta Biomater. 50 (2017) 546–555.
[127] R. Pörtner, C. Giese, An overview on bioreactor design, prototyping and process control for reproducible three-dimensional tissue culture, in: U. Marx, V. Sandig (Eds.), Drug Testing In Vitro: Breakthroughs and Trends in Cell Culture Technology, Wiley-Blackwell, 2007, p. 318.
[128] A. Quarteroni, Modeling the Heart and the Circulatory System, MS&A - Modeling, Simulation and Applications, Springer International Publishing, 2015, p. 238.
[129] K.F. Lorking, Inhibition of corrosion of magnesium in chromic acid, Nature 201 (4914) (1964), 75–75.
[130] I.M. Kolthoff, E.H. Vogelenzang, Le Titrage Acidimétrique du Bichromate, Recl. Trav. Chim. Pays Bas 40 (11) (1921) 681–685.
[131] ASM, Corrosion Resistance of Magnesium Alloys, Volume 13A Corrosion: Fundamentals, Testing, and Protection, ASM International, 2003.
[132] T.A. Hiller, V.A. Stenger, Determination of magnesium oxide in finely divided magnesium metal, Anal. Chem. 46 (13) (1974) 2019–2022.
[133] F. Feyerabend, 8-In vitro analysis of magnesium corrosion in orthopaedic biomaterials, in: P. Dubruel, S.V. Vlierberghe (Eds.), Biomaterials for Bone Regeneration, Woodhead Publishing, 2014, pp. 225–269.
[134] J. Kuhlmann, I. Bartsch, E. Willbold, S. Schuchardt, O. Holz, N. Hort, D. Höche, W.R. Heineman, F. Witte, Fast escape of hydrogen from gas cavities around corroding magnesium implants, Acta Biomater. 9 (10) (2013) 8714–8721.
[135] D. Zhao, T. Wang, J. Kuhlmann, Z. Dong, S. Chen, M. Joshi, P. Salunke, V.N. Shanov, D. Hong, P.N. Kumta, W.R. Heineman, In vivo monitoring the biodegradation of magnesium alloys with an electrochemical H2 sensor, Acta Biomater. 36 (Supplement C) (2016) 361–368.
[136] W.F. Ng, K.Y. Chiu, F.T. Cheng, Effect of pH on the in vitro corrosion rate of magnesium degradable implant material, Mater. Sci. Eng. C 30 (6) (2010) 898–903.
[137] W.A. Badawy, N.H. Hilal, M. El-Rabiee, H. Nady, Electrochemical behavior of Mg and some Mg alloys in aqueous solutions of different pH, Electrochim. Acta 55 (6) (2010) 1880–1887.
[138] C. Yang, G. Yuan, J. Zhang, Z. Tang, X. Zhang, K. Dai, Effects of magnesium alloys extracts on adult human bone marrow-derived stromal cell viability and osteogenic differentiation, Biomed. Mater. 5 (4) (2010), 045005.
[139] P. Lu, L. Cao, Y. Liu, X. Xu, X. Wu, Evaluation of magnesium ions release, biocorrosion, and hemocompatibility of MAO/PLLA-modified magnesium alloy WE42, J. Biomed. Mater. Res. Part B Appl. Biomater. 96 (1) (2011) 101–109.
[140] J. Walker, S. Shadanbaz, T.B.F. Woodfield, M.P. Staiger, G.J. Dias, Magnesium biomaterials for orthopedic application: a review from a biological perspective, J. Biomed. Mater. Res. Part B Appl. Biomater. 102 (6) (2014) 1316–1331.
[141] Z.G. Huan, M.A. Leeflang, J. Zhou, L.E. Fratila-Apachitei, J. Duszczyk, In vitro degradation behavior and cytocompatibility of Mg–Zn–Zr alloys, J. Mater. Sci. Mater. Med. 21 (9) (2010) 2623–2635.
[142] J.-H. Jo, B.-G. Kang, K.-S. Shin, H.-E. Kim, B.-D. Hahn, D.-S. Park, Y.-H. Koh, Hydroxyapatite coating on magnesium with MgF2 interlayer for enhanced

corrosion resistance and biocompatibility, J. Mater. Sci. Mater. Med. 22 (11) (2011) 2437–2447.
[143] V. Chavagnac, J.A. Milton, D.R.H. Green, J. Breuer, O. Bruguier, D.E. Jacob, T. Jong, G.D. Kamenov, J. Le Huray, Y. Liu, M.R. Palmer, S. Pourtalès, I. Roduhskin, A. Soldati, C.N. Trueman, H. Yuan, Towards the development of a fossil bone geochemical standard: an inter-laboratory study, Anal. Chim. Acta 599 (2) (2007) 177–190.
[144] T.H. Darrah, Inorganic Trace Element Composition of Modern Human Bones : Relation to Bone Pathology and Geographical Provenance, Dept. of Earth and Environmental Sciences, University of Rochester, 2009, p. 324.
[145] J.E. Abele, The physical background to freezing point osmometry and its medical-biological applications, Am. J. Med. Electron. 2 (1963) 32–41.
[146] R. Willumeit, J. Fischer, F. Feyerabend, N. Hort, U. Bismayer, S. Heidrich, B. Mihailova, Chemical surface alteration of biodegradable magnesium exposed to corrosion media, Acta Biomater. 7 (6) (2011) 2704–2715.